J Bio Tribo Corros (2017) 3:40
DOI 10.1007/s40735-017-0101-4

Human Osteoblast Cell-Ti6Al4V Metal Alloy Interactions Under Varying Cathodic Potentials: A Pilot Study

Arghya K. Bishal[1] · John Grotberg[1] · Cortino Sukotjo[2] · Mathew T. Mathew[3] · Christos G. Takoudis[1,4]

Received: 31 May 2017 / Revised: 23 June 2017 / Accepted: 8 July 2017 / Published online: 17 July 2017

Abstract Surface oxide plays an important role in the biocompatibility of metallic implants. The stability of this surface oxide varies depending on the surrounding environment of the implant. Numerous electrochemical processes may take place during formation and depletion of an oxide layer on the surface through corrosion. This shifts the open circuit potential (OCP) of titanium alloy (generally at ~150 mV vs. SCE) to be more cathodic. Therefore, the relation between cellular response and cathodic potential was investigated in this study first time for the MG63 cells type on the Ti-6Al-4V surface. Initially, the surface was polished and brought to a mirror finish. Then cells were cultured on top of such surfaces kept at two different static cathodic potentials (−300 and −600 mV vs. SCE) for 24 h. The experiments were facilitated using a custom glass corrosion chamber. With shifts toward more cathodic potentials than OCP, it was found that the well-spread viable cells rendered to small, rounded-up, unhealthy cells. This study suggested the apoptotic MG63 cell death due to electrochemical reactions and their products generated under cathodic potentials.

✉ Christos G. Takoudis
takoudis@uic.edu

[1] Department of Bioengineering, University of Illinois at Chicago, Chicago, IL, USA

[2] Department of Restorative Dentistry, College of Dentistry, University of Illinois at Chicago, Chicago, IL, USA

[3] Department of Orthopedic Surgery, Rush University Medical Center, Chicago, IL, USA

[4] Department of Chemical Engineering, University of Illinois at Chicago, Chicago, IL, USA

Keywords Surface oxide · Ti-6Al-4V · Open circuit potential (OCP) · MG63 cells · Cathodic potentials · Biocompatibility

1 Introduction

Metallic biomaterials are used extensively in the body to improve and restore the functions of different body parts [1, 2]. In particular, metals are widely used in dental and orthopedic implants for their superior mechanical properties, e.g., toughness and hardness, over any other class of materials [3]. However, many factors contribute to the success of a metallic implant like its ability to bear the cyclic load, minimize corrosion and resist wear conditions [4]. Metallic implants also face different challenges including lack of osseointegration [5], infection [6] and corrosion [7, 8]. Among these, osseointegration, the ability of the surrounding tissue to integrate with the surface of the metal implant, is one of the biggest concerns for metallic biomaterial [9]. Corrosion also plays a significant role in the biocompatibility of the metal alloy since surrounding cells are very sensitive to electrochemical reactions and the products generated during corrosion. Generally, metallic implants start corroding when they get exposed to cyclic load along with the corrosive environment inside the body. This may cause an adverse effect on the osseointegration and also on the mechanical stability of the implant [8–10]. Ultimately, the implant may fail from aseptic loosening due to the metal ion and wear debris released during corrosion. In order to improve the performance of metallic implants overcoming these modes of failure, a better understanding of the electrochemistry of corrosion and its effect on biocompatibility is very important.

Corrosion is a natural phenomenon by which the refined metals try to go back to their more stable form. In this process, a metal chemically reacts with the environment and thus gradually loses materials (metal oxide, metal ions). Therefore, higher resistance to corrosion is one of the most desired properties for a biocompatible metallic implant. Titanium and its alloys are widely used in dental and orthopedic implants due to their remarkable biocompatibility with bone tissue. Higher corrosion resistance is one of the main contributing factors behind this excellent biocompatibility of titanium and its alloys. Upon exposure to solution/air environment, a thin passive oxide layer is formed spontaneously on the top of these metal surfaces. This thin oxide film on its surface acts as a kinetic barrier to prevent corrosion [11]. However, this protective oxide layer may abrade away mechanically by adjacent bone or metal during fretting. Consequently, the metal surface tries to repassivate by protective oxide layer formation and this repassivation process induces many electrochemical events including a shifting of open circuit potential (OCP) of titanium (lies between −250 and −100 mV vs. Ag/AgCl) to more cathodic potentials [11]. Previous reports showed that the OCP of titanium and its alloy could drop to as low as −850 to −1000 mV versus SCE or lower under conditions of severe mechanical abrasion [12–14]. Such electrical polarization may have negative effects on the surrounding tissue. Therefore, it is important to know the influence of cathodic potentials on the biocompatibility of titanium alloy.

Previously, people have studied MC3T3 pre-osteoblast cell response on electrically polarized CoCrMo alloy [15, 17], commercially pure titanium (cpTi) [11, 18], anodized cpTi [16] and Ti-6Al-4V [4] surface as presented in Table 1. They reported a significant reduction in biocompatibility when those metal/alloys are held at cathodic potentials. Ehrensberger et al. [11] showed that application of a static cathodic potential of −600 and −1000 mV versus Ag/AgCl over 24 h caused ∼85% reduction in spreading and viability of pre-osteoblast cells cultured on the cpTi surface. Haeri et al. [16] reported a reduction below 5% in the viability of pre-osteoblast cells cultured on cpTi held at static cathodic potentials of −400 or −500 mV versus Ag/AgCl. Another work by Sivan et al. [4] reported the voltage threshold and time dependence of Ti-6Al-4V biocompatibility. In their work, they showed that cell death of pre-osteoblast cells resulted within 4 h at the cathodic polarization of −600 and −1000 mV versus Ag/AgCl while cell death occurred in 10–24 h at −400 mV versus Ag/AgCl. Recently, Ciolko et al. [18] examined the effect of applying periodic cathodic potential on the biocompatibility of cpTi, and they found significant reduction in viability and morphology of pre-osteoblast at −1000 mV versus Ag/AgCl enforced periodically over 24 h while no deleterious effect on cellular response at periodic polarization of −750 mV versus Ag/AgCl. In our study, we investigated for the first time the behavior of human osteoblast MG63 cell line, on mirror-finished smoother Ti-6Al-4V surface electrically polarized at three different potentials. We studied changes in cell morphology with the shifting of OCP toward more cathodic potentials. Also, we measured different electrochemical parameters to understand the correlation between cell behavior and cathodic polarization.

2 Materials and Methods

2.1 Sample Preparation

Ti-6Al-4V alloy disks of 15 mm diameter and 3 mm thickness (Mac-Master Carr, Elmhurst, IL) were mechanically wet-ground using a series of abrasive pads (#320, #400, #600 and #800) (Carbimet 2, Buehler, Lake Bluff, IL). Samples were then polished using diamond paste (MetaDi 9-micron, Buehler, Lake Bluff, IL) with lubricant (MetaDi Fluid, Buehler, Lake Bluff, IL) on polishing cloth (TexMet polishing cloth, Buehler, Lake Bluff, IL), and brought to mirror finish using colloidal silica polishing suspension (MasterMet, Buehler, Lake Bluff, IL) on polishing cloth (Chemomet I, Buehler, Lake Bluff, IL). Samples were then washed with deionized water and sonicated in 70% ethanol. After that, samples were autoclaved followed by a wash with 70% ethanol prior to cell culture.

2.2 Osteoblast Cell Culture

MG63 human osteoblasts cells were cultured in Dulbecco's modified Eagle medium (DMEM) (Gibco) with 10% fetal bovine serum (FBS) (Gibco) and 1% antibiotic (Gibco) until roughly 80% confluence in a cell culture incubator at 37 °C and 5% CO_2. Cells were then trypsinized using 0.25% trypsin (Sigma) and subcultured for experimentation. Cells were seeded on the titanium alloy disks at a density of 1.15×10^5 cells per disk (with 1.13 cm^2 of available exposed area inside corrosion chamber) for 1 day prior to electrochemical testing.

2.3 Electrochemical Tests

Each titanium alloy disk seeded with cells was transferred to a custom glass corrosion apparatus (Fig. 1a). The disk was mounted at the bottom of this chamber. A stainless-steel screw was connected to the underside of the titanium alloy disk and passed through the Teflon threaded bushing to serve as an external electrical contact to the sample. A sterile O-ring was used in the threading between glass and

Table 1 Previous studies on effect of cathodic potentials on biocompatibility of metal implant materials

Metal/alloy	Cell type	Polarizing potentials (mV) versus Ag/AgCl	Significant findings	References
cpTi, grade 4	MC3T3-E1 pre-osteoblast	−1000 to +1000	−600 to −1000 mV dramatically reduced spreading and viability of cells	Ehrensberger et al. [11]
CoCrMo	MC3T3-E1 pre-osteoblast	−1000 to +500	Below −400 mV apoptotic cell death reported	Haeri et al. [15]
cpTi, grade 4 (bare and anodized)	MC3T3-E1 pre-osteoblast	−400 and −500	On anodized sample cells showed higher viability at −400 and −500 mV compared to bare sample	Haeri et al. [16]
Ti-6Al-4V	MC3T3-E1 pre-osteoblast	−600 to −300 mV	−400 mV is voltage threshold for cell viability, cell died below this potential, and this killing effect is also time dependent	Sivan et al. [4]
CoCrMo	MC3T3-E1 pre-osteoblast	−100, −400, −1000 and +500	For −1000 mV cell death can occur very quickly (~15 min), whereas for +500 and −400 it can take hours	Haeri and Gilbert [17]
cpTi, grade 2	MC3T3-E1 pre-osteoblast	−750 and −1000	Cell viability was reduced significantly at −1000 mV, while cells were viable at −750 mV	Ciolko et al. [18]

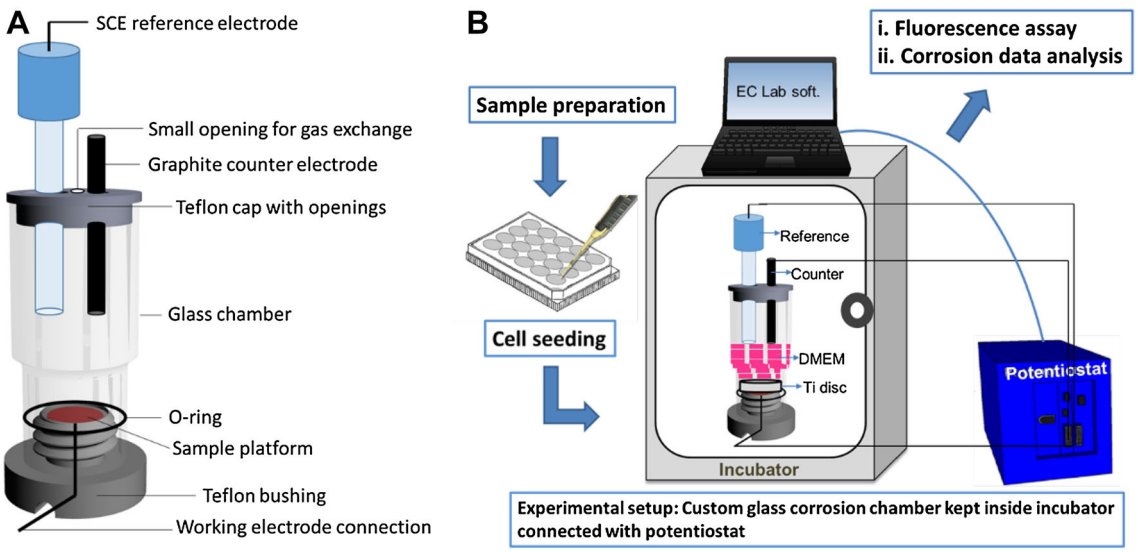

Fig. 1 **a** Schematic of custom-made glass electrochemical chamber, **b** schematic of the experimental setup

Teflon bushing to achieve a water-tight seal around the titanium alloy surface. 1.13 cm^2 of exposed area of the sample to the interior of the chamber is achieved in this setup. Another Teflon cap was used to seal the chamber from the top. This cap had openings for graphite counter electrode: CE, reference electrode: RE (in this case, Saturated Calomel Electrode or SCE) and for proper gas exchange from incubator environment. The sample served as the working electrode. Right after mounting the disk with the cell, the glass chamber was filled with 12 ml of cell culture DMEM to avoid any stress or shock to cells. Here the cell culture media served as the electrolyte for corrosion study, and the pH was 7.5 at room temperature. The entire experiment was performed inside an incubator at 37 °C to simulate physiologic temperature of the human body (Fig. 1b).

Electrochemical impedance spectroscopy (EIS) was performed at a range of 100 k–0.005 Hz, prior to 24 h of potentiostatic polarization. A potentiostat (SP-240, Bio-Logic, Claix, France) was used for application of static potentials. Two different cathodic potentials were examined during this study, i.e., −300 mV versus SCE, −600 mV versus SCE, and open circuit potential (no applied potential) was used as a control (Fig. 2a). Since previous reports (Table 1) indicated that −400 mV might be a viability threshold and below that (i.e., <−400 mV) a dramatic reduction of cell spreading and viability for MC3T3-E1 mouse pre-osteoblast cells seeded on Ti and its

alloy surface would take place, the two potentials −300 and −600 mV were chosen for MG63 human osteoblast cell responses. For our case, OCP was between −250 and −135 mV versus SCE. Finally, after 24 h of potentiostatic polarization, EIS was performed again at the above-mentioned frequency range and at OCP. The sequence of corrosion protocol is displayed in Fig. 2b.

Additionally, EIS data were used to estimate total polarization resistance and capacitance using constant phase element (CPE) equivalents. A modified Randle's circuit (Fig. 2c) was used to model the impedance. EC-Lab version 10.23 software was used to perform the z-fit analysis of this equivalent circuit model over a range of 1000–0.01 Hz. Bode and Nyquist plots were used to calculate the solution resistance (R_s), polarization resistance (R_p or R film), constant phase element (CPE) and alpha (n). All these values were measured before and after 24 h of potentiostatic polarization. Following the electrochemical test, the electrodes were disconnected from the potentiostat and then the samples were prepared for fluorescence assay.

2.4 Fluorescence Assay

Cell morphology on each sample group was assessed after 24 h of electrochemical tests using fluorescent dye-based reagent labeling (Molecular Probes™, ThermoFisher Scientific) and fluorescence microscopy. Cells were imaged with a fully automated inverted microscope (Leica DMI6000 B, Leica Microsystem, Germany), and post-processing of the images was performed using LAS AF software (Leica, Germany). Prior to imaging, cells were first fixed in 3.7% formaldehyde, permeabilized with 0.1% Triton X-100 and stained in phosphate-buffered saline (PBS). Actin and nuclei were stained with ActinRed™ 555 ReadyProbes® Reagent (Molecular Probes™, ThermoFisher Scientific) and NucBlue® Fixed Cell ReadyProbes® Reagent (Molecular Probes™, ThermoFisher Scientific), respectively.

3 Results

3.1 Cell Morphology

Fluorescence images of MG63 cells cultured on Ti-6Al-4V alloy samples, electrically polarized at the three different potentials (OCP, −300, −600 vs. SCE) for 24 h, are displayed in Fig. 3. Cellular morphology was found to be affected by cathodic voltages depending on their magnitude. The morphology of cells cultured on control sample maintained freely at OCP was well spread and higher in density compared to the other two potentials shown in Fig. 3. The size of the cells cultured at −300 mV did not differ from the cells maintained at OCP. In spite of being less dense

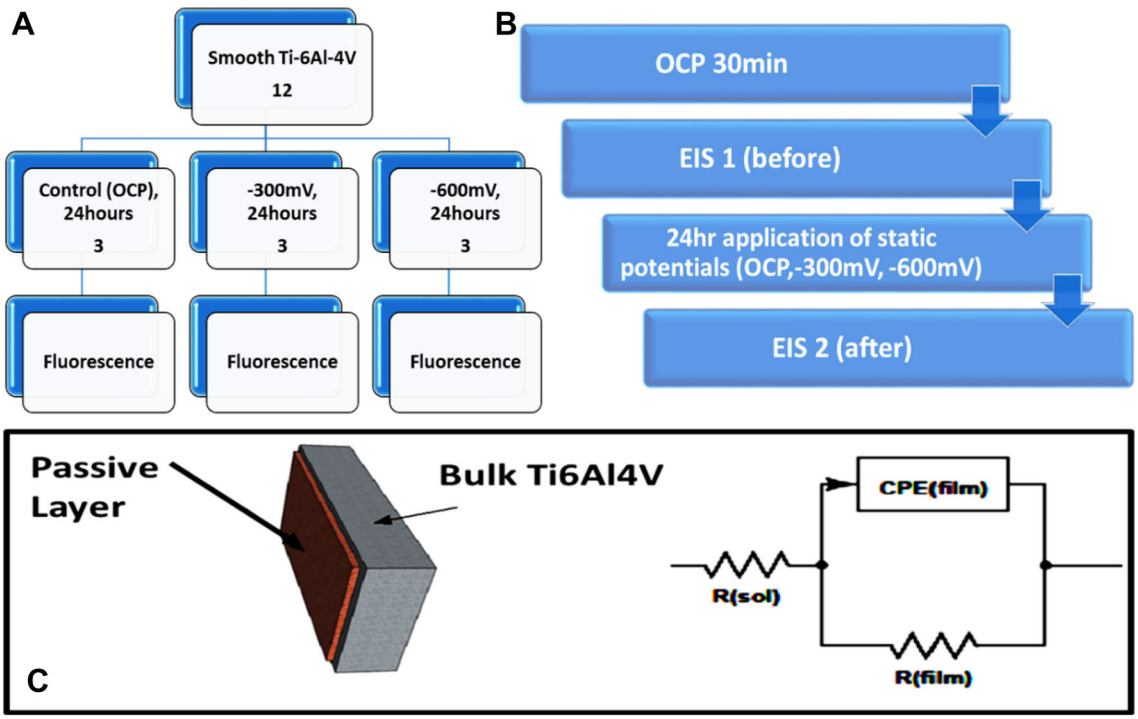

Fig. 2 **a** Schematic of experimental design, **b** diagram of corrosion protocol used, **c** schematic of modified Randle's circuit used for modeling electrochemical impedance, where R (sol) represents the resistance of the solution and CPE (film) and R (film) represent the capacitance and resistance of the native oxide film, respectively

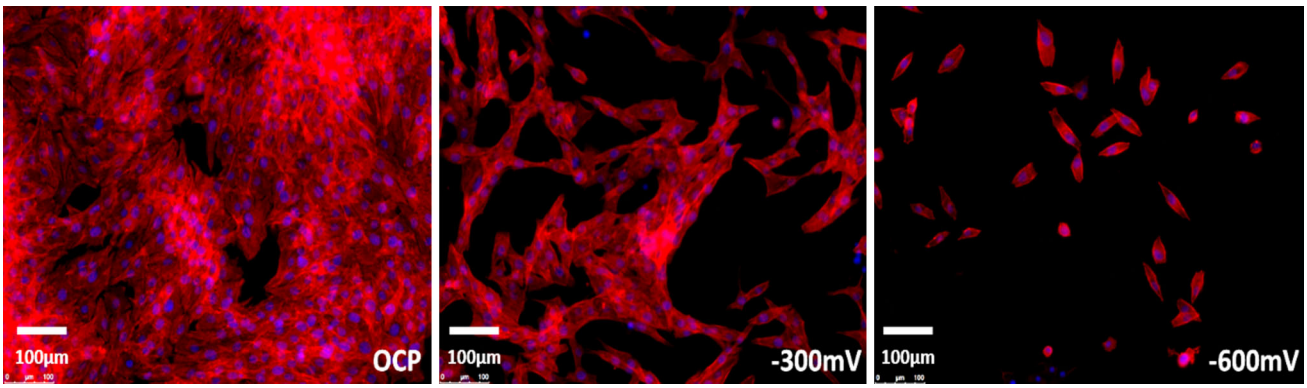

Fig. 3 Fluorescence image of cell morphology after 24 h of different potential applications

compared to OCP, the cells cultured at −300 mV remained elongated and well spread with clear evidence of flattened actin and the presence of nuclei. However, a stark difference in the morphology of cells cultured at −600 mV was observed from the cell morphology at −300 mV and OCP. Cells cultured on the samples polarized at −600 mV were rendered small, balled up and fewer in number. Thus, Fig. 3 reveals clear differences in cell morphology of MG63 cells due to the application of different potentials.

3.2 Electrochemical Current Density

The average current densities the MG63 cells experienced over a period of 24 h when they were cultured on Ti-6Al-4V polarized at different potentials are presented in Fig. 4. These cathodic current densities were found to be increased with the cathodic shift of the applied potential. Current values measured at −300 mV were $\sim 3\times10^{-4}$ mA·cm^{-2}. Larger current values of $\sim 6.8 \times 10^{-4}$ mA·cm^{-2} were measured at −600 mV, and cells became small size and balled up at this low reduction current density.

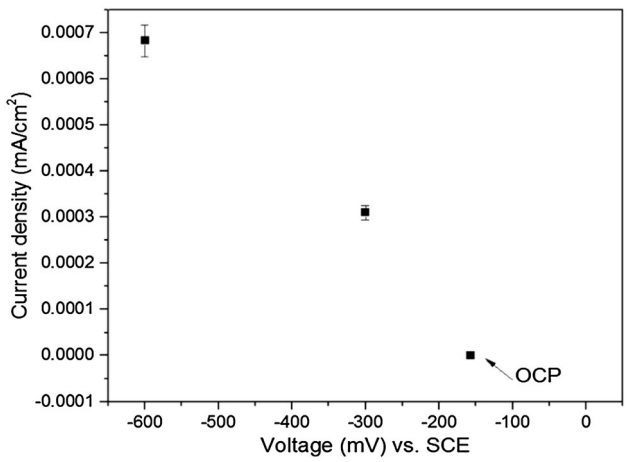

Fig. 4 Current evolution due to application of potentials for 24 h

3.3 Electrochemical Impedance Analysis

To analyze the electrochemical events at the surface oxide layer and to find a correlation of the observed cellular responses with those events, electrochemical impedance spectroscopy (EIS) was employed. Impedance spectra were recorded before and after 24 h of polarization, and the EIS results at OCP, −300 and −600 mV versus SCE have been presented as Bode plots (phase angle vs. frequency and impedance|z| vs. frequency) in Fig. 5a, b and as Nyquist plot (real Z vs. img Z) in Fig. 6. For each experimental condition, all the representative Bode plots showed single time constant behavior. No significant change in the impedance spectra and in the phase angles was observed before 24 h or at the start of polarization among the three potentials used. However, changes were observed after 24 h of polarization with static potentials. As shown in Fig. 5b, the impedance drops with shifting toward more cathodic potentials from OCP. The phase angle was also found to get lowered with a cathodic shift of potentials at frequency ranges from 1 to 100 Hz. Bode plots did not show the drop of impedance very clearly though.

A significant drop in impedance is observed more clearly in Nyquist plot (Fig. 6) with the cathodic shift in potentials. The Nyquist plots for all the three potentials were subsequently fit to a modified Randles circuit. The values of total polarization resistance (R_p or R film), constant phase element (CPE or capacitance) and alpha for samples at OCP, −300 and −600 mV versus SCE are displayed in Fig. 7.

There was a noticeable reduction in R_p after 24 h for the samples statically polarized at −300 and −600 mV versus SCE compared to the samples maintained at OCP. On the other hand, the capacitance values determined for the samples at −300 and −600 mV versus SCE were larger compared to the OCP. The alpha value (CPE exponent) for the samples polarized at −300 and −600 mV versus SCE was smaller than the alpha value of the sample maintained at OCP. The resistance of the solution (R_s) did not change

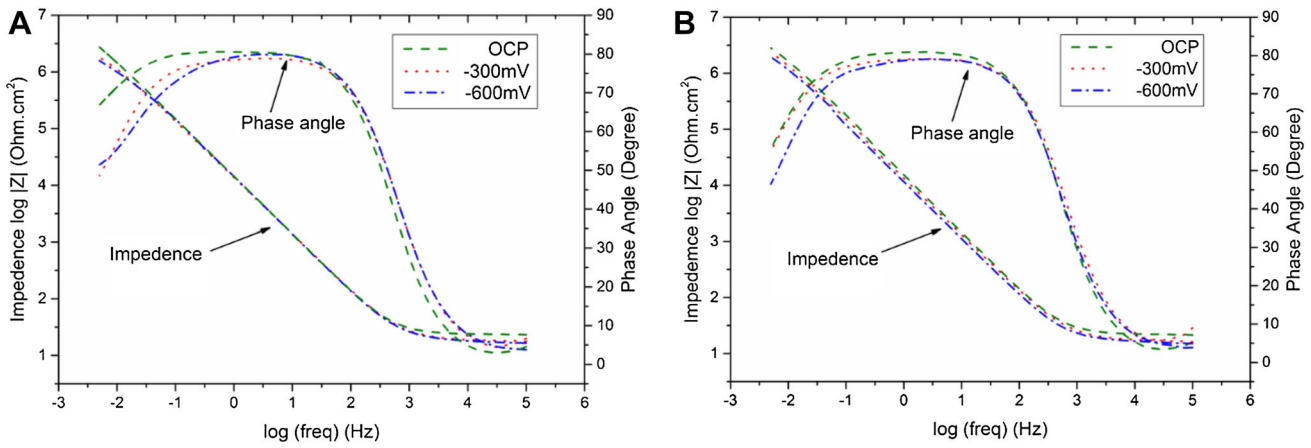

Fig. 5 Bode plot before (**a**) and after (**b**) 24 h of polarization

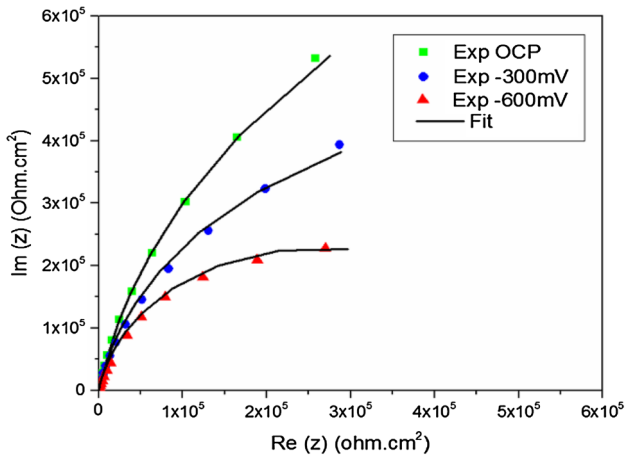

Fig. 6 Nyquist plot of three potentials with fitted curve after 24 h of polarization

significantly across all the potentials, and it remained $\sim 15.7\ \Omega{\cdot}cm^2$.

4 Discussion

The results of this study have demonstrated that static cathodic potentials have a negative impact on the MG63 cell morphology cultured on the smooth Ti-6Al-4V surface within 24 h. The cell morphology observed at OCP can be related to the cell condition in the normal cell cycle where the cells are well spread and healthy. Shifting of OCP toward more cathodic voltages resulted in a reduction of the cell morphology and viability. −300 mV versus SCE voltage range seemed to be the borderline between healthy, fully spread cells and unhealthy, balled-up cells. Significant reduction in cell spreading was observed at −600 mV versus SCE where the cells became small and rounded. This reduced biocompatibility of MG63 cells observed due to the application of static cathodic potential is consistent with previous reports for different cell types. Shivan et al. and Ehrensberger et al. [4, 11] reported a similar trend in the reduction of biocompatibility for MC3T3 pre-osteoblast cell lines cultured on the Ti-6Al-4V surface and cpTi surface, held at static cathodic potentials for 24 h. The periodic cathodic polarization of cpTi was also reported to reduce viability and morphology of MC3T3 pre-osteoblast significantly over 24 h [18]. This negative effect of cathodic potential on pre-osteoblast cellular behavior is not only limited to titanium and its alloys. In the case of CoCrMo alloy (OCP lies between −200 and −400 mV vs. Ag/AgCl), it has also been reported that MC3T3 pre-osteoblast cells became rounding up, reduced size and finally non-viable below −400 mV (Ag/AgCl) [15].

This observed cellular viability throughout the voltage range can be correlated with the cathodic current densities. Low current density (3×10^{-4} mA·cm^{-2}) was recorded for voltages within a viable range where cells are well spread. At −600 mV versus SCE, a relatively larger cathodic current density (6.8×10^{-4} mA·cm^{-2}) was measured which likely attributed to the significant reduction in cell spreading. Ciolko et al. [18] reported that the large cathodic current density increases oxygen consumption in the adjacent microenvironment of the polarized metal surface, as oxygen reduction is the dominant cathodic half-cell reaction for these experimental conditions. Gilbert et al. [13] also reported a reduction in cell spreading and viability as consequence of a local depletion of oxygen adjacent to the cathodically polarized cpTi surface at −1000 mV versus Ag/AgCl. Therefore, the observed reduction in cell spreading in our study could be due to depletion of oxygen. Additionally, Kalbacova et al. [19] have shown that production of intracellular reactive oxygen species (ROS) increases by application of cathodic current densities ranging from −0.5 to −5 μA·cm^{-2} to Ti-6Al-4V for 24 h and this ROS reduces metabolic activity

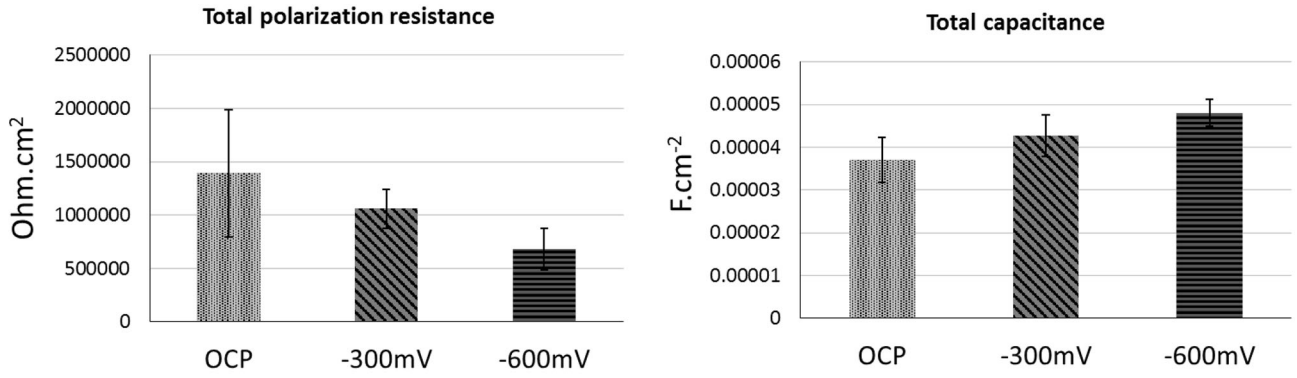

Potential conditions	R_p (Ω.cm^2)	CPE (F.cm^{-2})	Alpha
OCP	13.93±5.97×10^5	3.7±0.52×10^5	0.929±0.014
-300mV	10.58±1.79×10^5	4.27±0.48×10^5	0.874±0.007
-600mV	6.8±1.93×10^5	4.8±0.31×10^5	0.892±0.012

Fig. 7 EIS fitting results: polarization resistance (*top left*), total capacitance (*top right*), and summary of resistance, capacitance and alpha values at different potential conditions (*bottom*)

of osteoblast-like cells. This could be another contributing factor to the reduction in cell spreading on the cathodically polarized Ti-6Al-4V surface.

The electrochemical conditions and properties of the surface were also found to be closely followed by the cellular response of MG63 on the polarized Ti-6AL-4V surface. For all the sample groups, the film resistance (R_p) and capacitance (CPE) values changed significantly after 24 h of application of cathodic potentials. The impedance outcome of this study demonstrated that the sample held at static −600 mV versus SCE potential had relatively small R_p value ($6.8 \pm 1.93 \times 10^5$ Ω·cm^2) as compared to the film resistance values of the samples kept at OCP and −300 mV versus SCE. On the other hand, capacitance value ($4.8 \pm 0.31 \times 10^5$ F·cm^{-2}) was highest at −600 mV versus SCE compared to all the other experimental conditions. This decreased resistance and increased capacitance conditions of the sample held at −600 mV clearly indicate the high conductivity of the surface oxide and thereby thinning of surface oxide film over time. The resistance and capacitance of an oxide can also be determined from the following general equations [18]:

$$\text{Resistance of oxide } (R_{ox}) = \frac{L\rho}{A}$$

$$\text{and Capacitance of oxide } (C_{ox}) = \frac{k\epsilon_0 A}{L},$$

where L is oxide thickness, ρ is oxide resistivity, A is a cross-sectional area, k is dielectric constant, and ε_0 is the permittivity of free space. Considering the titanium dioxide resistivity value as $\sim 10^8$ Ω·cm and from the measured resistance values of the oxide, the calculated thickness values of the surface oxide film for OCP, −300 and −600 mV are 0.16, 0.12 and 0.07 mm, respectively. Therefore, these equations show the thinning of oxide layer due to a decrease in resistance and increase in capacitance, as we found for the sample at −600 mV. This finding is consistent with previous reports on different cell lines, where they showed the generation of an electrochemical interface with lower resistance and higher capacitance as a result of applying cathodic potentials [11, 18, 20]. This unstable thin oxide layer could be another contributing factor to the deleterious cell response of MG63 at −600 mV versus SCE. However, OCP and −300 mV had relatively higher R_p and lower capacitance which offered a stable, biocompatible surface oxide layer favorable for healthy and well-spread cell morphology (Fig. 8).

Cathodic potentials may also induce reduction reactions and thereby generation of toxic compounds like hydrogen peroxide [4, 15]. Generation of hydrogen peroxide was reported on titanium oxide surface under cathodic voltage in oxygen-containing aqueous solutions [21]. This hydrogen peroxide generation can lead to oxidative stress which can affect cell functionality like cellular adhesion [22]. Therefore, either one of this mentioned reaction or the cumulative contribution of all can be responsible for such deleterious effect on our MG63 cell morphology cultured on the cathodically polarized Ti-6Al-4V surface.

Now, apart from the electrochemical reasons behind cell death, the biological pathway or the mechanism responsible for cell death may also be an important factor for consideration. Haeri et al. [15] described the cell death by two distinguishable mechanisms, either through apoptosis

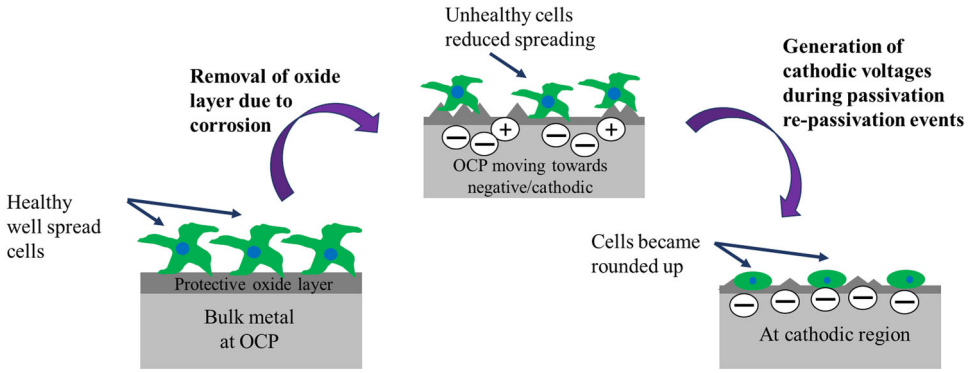

Fig. 8 Schematic diagram of corrosion-induced cathodic potentials' impact on cell spreading. At early stage, metal surface has a protective and biocompatible native oxide layer on the surface keeping the cells viable and well spread; with the removal of oxide layer due to corrosion, OCP of the metal starts decreasing toward more cathodic region causing reduction in cell spreading, i.e., unhealthy cells

where modification in internal cell signaling pathway causes death or through necrosis where disruption-mediated cell death happens from sudden injury. They mentioned the high concentration release of capacase 3 and 9 protein as an indicator of cell death when MC3T3 pre-osteoblast was a culture on cathodically polarized (−400 and −500 mV) CoCrMo alloy surface. In our case, we observed the shrunken, oval-shaped, small cells at −600 mV and which may also be an indication of an apoptosis process.

5 Conclusion

We investigated the impact of the cathodic shift in potential of mirror-finished Ti-6Al-4V surfaces on human osteoblast MG63 cells. We observed healthy well-spread cells on Ti-6Al-4V surfaces held at OCP and −300 mV versus SCE, while at −600 mV versus SCE the cells started shrinking and becoming smaller in number and finally becoming balled up due to a remarkable reduction in cell spreading. The cellular behavior closely followed electrochemical events at the surface. At −600 mV, the observed highest capacitance and lowest resistance suggested an unstable surface oxide layer attributed to a reduction in cell morphology. At −600 mV, we also observed relatively large cathodic current density which might be another factor contributing to the reduction of cell spreading. This apparent deleterious effect of the cathodically polarized surface on cell morphology could be apoptotic in nature. However, there could be a lot of other factors responsible for cell death. This type of cellular response on the electrically polarized surface may also not be limited to particular cell type or metal type. Further investigation is required for an in-depth understanding of the dominating mechanism behind the reduction in cell spreading and survivability. As Ti-6Al-4V is a widely used alloy in orthopedic and dental clinical practices, our finding has a promising clinical significance in addressing the challenges related to in vivo osseointegration.

Acknowledgements We are very thankful to Richard Frueh, Physical Sciences Machine Shop, UIC Department of Physics, Brian D. Schwandt, Glass shop, UIC Department of Chemistry, for their aid and assistance in designing the corrosion chamber for this work, and the National Science Foundation (CBET #1067424 and DMR #1307052) for the financial support.

Compliance with Ethical Standards

Conflict of interest On behalf of all authors, the corresponding author states that there is no conflict of interest.

References

1. Pohler OE (2000) Unalloyed titanium for implants in bone surgery. Injury 31:D7–D13
2. Wintermantel E, Ha S-W (2008) Medizintechnik: life science engineering. Springer, Berlin
3. Navarro M, Michiardi A, Castano O, Planell J (2008) Biomaterials in orthopaedics. J R Soc Interface 5(27):1137–1158
4. Sivan S, Kaul S, Gilbert JL (2013) The effect of cathodic electrochemical potential of Ti-6Al-4V on cell viability: voltage threshold and time dependence. J Biomed Mater Res B Appl Biomater 101(8):1489–1497
5. Keegan GM, Learmonth ID, Case C (2008) A systematic comparison of the actual, potential, and theoretical health effects of cobalt and chromium exposures from industry and surgical implants. Crit Rev Toxicol 38(8):645–674
6. Spangehl MJ, Younger A, Masri B, Duncan C (1998) Diagnosis of infection following total hip arthroplasty. Instr Course Lect 47:285–295
7. Gilbert J (2011) Electrochemical behavior of metals in the biological milieu. Compr Biomater 1(1):103
8. Jacobs JJ, Gilbert JL, Urban RM (1998) Current concepts review-corrosion of metal orthopaedic implants*. J Bone Joint Surg 80(2):268–282

9. Gittens R, Olivares-Navarrete R, Tannenbaum R, Boyan B, Schwartz Z (2011) Electrical implications of corrosion for osseointegration of titanium implants. J Dent Res 90(12): 1389–1397
10. Gilbert JL, Mehta M, Pinder B (2009) Fretting crevice corrosion of stainless steel stem–CoCr femoral head connections: comparisons of materials, initial moisture, and offset length. J Biomed Mater Res B Appl Biomater 88(1):162–173
11. Ehrensberger MT, Sivan S, Gilbert JL (2010) Titanium is not "the most biocompatible metal" under cathodic potential: the relationship between voltage and MC3T3 preosteoblast behavior on electrically polarized cpTi surfaces. J Biomed Mater Res A 93(4):1500–1509
12. Contu F, Elsener B, Böhni H (2004) A study of the potentials achieved during mechanical abrasion and the repassivation rate of titanium and Ti6Al4V in inorganic buffer solutions and bovine serum. Electrochim Acta 50(1):33–41
13. Gilbert JL, Zarka L, Chang E, Thomas CH (1998) The reduction half cell in biomaterials corrosion: oxygen diffusion profiles near and cell response to polarized titanium surfaces. J Biomed Mater Res 42(2):321–330
14. Venugopalan R, Weimer JJ, George MA, Lucas LC (2000) The effect of nitrogen diffusion hardening on the surface chemistry and scratch resistance of Ti-6Al-4V alloy. Biomaterials 21(16):1669–1677
15. Haeri M, Wöllert T, Langford GM, Gilbert JL (2012) Electrochemical control of cell death by reduction-induced intrinsic apoptosis and oxidation-induced necrosis on CoCrMo alloy in vitro. Biomaterials 33(27):6295–6304
16. Haeri M, Wöllert T, Langford GM, Gilbert JL (2013) Voltage-controlled cellular viability of preosteoblasts on polarized cpTi with varying surface oxide thickness. Bioelectrochemistry 94:53–60
17. Haeri M, Gilbert JL (2013) Study of cellular dynamics on polarized CoCrMo alloy using time-lapse live-cell imaging. Acta Biomater 9(11):9220–9228
18. Ciolko AA, Tobias M, Ehrensberger MT (2015) The effect of fretting associated periodic cathodic potential shifts on the electrochemistry and in vitro biocompatibility of commercially pure titanium. J Biomed Mater Res B Appl Biomater 104(8): 1591–1601
19. Kalbacova M, Roessler S, Hempel U, Tsaryk R, Peters K, Scharnweber D, Kirkpatrick JC, Dieter P (2007) The effect of electrochemically simulated titanium cathodic corrosion products on ROS production and metabolic activity of osteoblasts and monocytes/macrophages. Biomaterials 28(22):3263–3272
20. Ehrensberger MT, Gilbert JL (2010) The effect of static applied potential on the 24-hour impedance behavior of commercially pure titanium in simulated biological conditions. J Biomed Mater Res B Appl Biomater 93(1):106–112
21. Clechet P, Martelet C, Martin J, Olier R (1979) Photoelectrochemical behaviour of TiO 2 and formation of hydrogen peroxide. Electrochim Acta 24(4):457–461
22. Chiarugi P, Pani G, Giannoni E, Taddei L, Colavitti R, Raugei G, Symons M, Borrello S, Galeotti T, Ramponi G (2003) Reactive oxygen species as essential mediators of cell adhesion the oxidative inhibition of a FAK tyrosine phosphatase is required for cell adhesion. J cell biol 161(5):933–944